

Citation for published version: Shen, Y, Gu, C, Xiang, Y, Fu, Y, Huo, D, Li, J & Zhao, P 2022, 'Dynamic Service Restoration for Integrated Energy Systems under Seismic Stress', *IEEE Transactions on Sustainable Energy*, vol. 13, no. 1, 9576820, pp. 527-536. https://doi.org/10.1109/TSTE.2021.3119179

DOI:

10.1109/TSTE.2021.3119179

Publication date: 2022

Document Version Peer reviewed version

Link to publication

© 2021 IEEE. Personal use of this material is permitted. Permission from IEEE must be obtained for all other users, including reprinting/ republishing this material for advertising or promotional purposes, creating new collective works for resale or redistribution to servers or lists, or reuse of any copyrighted components of this work in other works.

# **University of Bath**

# **Alternative formats**

If you require this document in an alternative format, please contact: openaccess@bath.ac.uk

Copyright and moral rights for the publications made accessible in the public portal are retained by the authors and/or other copyright owners and it is a condition of accessing publications that users recognise and abide by the legal requirements associated with these rights.

**Take down policy**If you believe that this document breaches copyright please contact us providing details, and we will remove access to the work immediately and investigate your claim.

Download date: 07 Mar 2023

# Dynamic Service Restoration for Integrated Energy Systems under Seismic Stress

Yichen Shen Student Member, Chenghong Gu, Member, IEEE, Yue Xiang, Seinor Member, IEEE, Yang Fu, Da Huo, Junlong Li Student Member, IEEE, Pengfei Zhao, Student Member, IEEE

Abstract—Seismic events and aftershocks can cause devastating impacts on overground and underground energy system infrastructure. This paper designs a novel approach to restore energy system functionality in response to seismic stresses by using coordinated dynamic system reconfiguration and operation. First, the impact of seismic stresses on system infrastructure is evaluated, considering critical system components, including electricity lines, substations, gas pipes, and operable units including combined heat pump (CHP), electrolyser, soft open point (SOP), energy storage units. Load curtailment is assumed to be caused by system branch overloading, reversed gas flows, and isolated branches. The objective of the proposed operation method is to maximize overall system restoration capability. Responding to seismic stresses and aftershocks, storage, SOPs and coupling components are dynamically operated to restore both gas and electricity supply thus reducing losses. A service index is quantified by considering both load curtailment and recovery time. A representative integrated electricity and gas system is employed to demonstrate the effectiveness of the proposed method. Results illustrate that the adverse impact of seismic stresses can be effectively reduced with the proposed model. This work provides system operators a powerful tool to restore the functionality of energy systems under seismic events, helping maintain supply security.

Index Terms—seismic events, Operation, Integrated electricity and gas system, Service restoration

	Nomenclature
$P_i$	The probability of $i$ th leak scenarios.
$d_i$	Equivalent orifice diameter under the $i$ th
	damage scenarios.
EOD	Equivalent orifice diameter
t	Thickness of maximum possible annular
	space.
k	Annular disengagement constant of
	damaged pipes.
$k_{1}, k_{2}$	Local crack constant of pipe wall.
$\theta$	Opening angle of damage orifice.
D	Diameter of the damaged pipe.
w	Width of split of damaged pipe.

<sup>&</sup>lt;sup>1</sup> Yichen Shen (ys884@bath.ac.uk) and Chenghong Gu (corresponding author: cg277@bath.ac.uk), Junlong Li are with the University of Bath, Bath, UK; Yue Xiang is with Sichuan University, China; Yang Fu is with Shanghai University of Electric Power, Shanghai, China; Da Huo is with Cranfield, UK; and Pengfei Zhao is with Chinese Academy of Sciences, Beijing ,China..

$L_{line}$ , $L_{Buck}$ ,	The overloading line, tower <sup>1</sup> buckling
$L_{iso}$	and isolated load induced load
	curtailment
D, F	The kth failure scenario related damaged
	and functional branches
$Pbest_i$	The <i>i</i> th particle's recorded best position
$Gbest_i$	The entire population's recorded best
	position
$V_i^t$	The <i>i</i> th Particle's velocity at time t
$x_i^t$	The <i>i</i> th Particle's position at time t
α	The stochastic acceleration terms's
	inertia weights
$eta_1,eta_2$	The stochastic acceleration terms'
	weighting factors
$r_1, r_2$	Randomly chosen numbers from a
	uniform distribution [0,1]
$I_c, V_c$	System branches' current and voltage
	constraints
$S(V_i)$	Sigmoid limiting transformation
$LL_{rev}$	Reversed pipes induced load curtailment
$DF_j^t$	Pipe flow direction at time t
$P_c$	Pipe pressure constraint
$F_{c}$	Pipe flow constraint
$E_{PtG}$ , $E_{GtP}$	Power to gas energy transformation and
	Gas to power energy transformation
A	Gas network connection matrix
G	Pipes admittance matrix
Q	Gas nodes flow rate vectors

# I. INTRODUCTION

THE integration of various energy vectors, particularly electricity and natural gas systems, has widely grown in recent years. Many technologies, for instance, combined heat and power (CHP), energy hubs, and electrolysis, enable the increasing coupling of the different energy infrastructure, improving system flexibility and reliability. In the meantime, due to climate change, natural events with low probability but high impact, such as storms, flooding, extreme precipitation,

heat waves, could cause severe damages to integrated energy systems. The consequence of failures in one energy system could propagate to other energy systems, causing significant cascading energy losses. Thus, the security of integrated electricity and natural gas systems under extreme natural events should be better managed from an integrated perspective.

Because of the growing coupling of integrated gas and electricity systems (IEGS), more attention from both academia and industry is dedicated to their optimal planning and scheduling operation. Paper [1] presents an interdependency modelling method for IEGS from the perspective of electricity and gas companies. Based on power-to-gas facilities, the operation strategies of bi-directional energy flows in IEGS are studied in [2]. Consequently, a multi-state model is proposed to evaluate the reliability of IEGS based on universal generating function techniques [3, 4]. These functions are aggregated to obtain the multi-state models of gas networks. The interdependency of IEGS can also make it more vulnerable. For instance, gas source outages or pipeline contingencies may cause the interruption of gas supply [5]. Subsequently, gas plants that cannot obtain sufficient gas should dramatically reduce power output, disturbing the supply services of electricity systems. Considering the increasing complexity of IEGS, the scheduling operation considering both inner and outer threats should be investigated.

Due to that seismic activities can damage both overground and underground parts of energy systems, it is essential to study how integrated energy systems behave and react to seismic activities. The seismic intensity can be quantified by peak ground velocity (PGV), and peak ground acceleration (PGA). From the topological point of view, papers [6, 7] quantify the seismic impact on integrated electricity and gas systems in terms of connectivity loss and power loss. Based on that, further research [8] shows that, compared to separate electricity and gas networks, the interdependency of gas and electricity systems shows an increased vulnerability. Consequently, to promote system security, the response and behaviours of integrated gas and electricity should be investigated.

With various types of switches, distribution electricity system topology can be easily reconfigured. Distributed generators and energy storage can be scheduled to restore system functionality. Normally, distribution systems are operated in a radial configuration, where switches can be employed to offer efficient protection schemes and fast fault isolation. An emergency restoration method is proposed in [9] to provide an emergency power supply to critical load in extreme natural catastrophes. A self-recovery method that sectionalizes distribution systems into microgrid is presented in [10]. The outage portions of distribution systems are optimally sectionalized into self-supplied microgrids, and then operable components are rescheduled to supply maximum load. The cumulative supply interruption durations of customers can be minimized by optimally scheduling available crews [11]. To solve this problem, repair and restoration are modelled as a scheduling problem with soft precedence constraints. In [12-15], optimization models based on an optimal power flow model are implemented, where the maximum number of switching statuses (ON/OFF) is specified by network operators. The lines

that should be switched to optimally improve the resilience of the power system are defined as decision variables in operational planning. However, the research can only offer resilience enhancement before or after a large disturbance for a short period. For a typical natural disaster that may last for a few days or even longer, system damage cannot be recovered without repair. Regarding seismic stress and aftershocks, one of the solutions can be dynamic reconfiguration and operation.

This paper proposes a new combined reconfiguration and operation method to restore the supply services for integrated energy systems to effectively mitigate load losses and recovery time under seismic stresses. IEGS is sectionalized and reconfigured by using natural gas valves, switches, and Soft Open Points(SOP). Energy storage, Combined heat pump (CHP) and Electrolyser are operated to maximize supply during the stresses. The reconfiguration of IEGS and operation of all operable units is formulated as a convex problem. To evaluate the efficiency of the proposed method, a service index that reflects both load losses and system recovery time is proposed. An integrated 33-bus and 13-gas-node IEGS is used to verify the proposed method. Results illustrate that load curtailment and system recovering time can be significantly reduced.

The main contributions of this paper are:

- Due to the lack of studies in service restoration of IEGS under seismic stresses, this paper presents a system operation method by operating switches/valves, electric/gas storage, CHP and electrolyser to restore supply service under seismic stresses for IEGS.
- Based on the coordination of both electricity and gas systems, it proposes a new dynamic reconfiguration scheme for IEGS to reduce load curtailment and recovery time.
- It designs a comprehensive service index that considers both system damage and recovery time to more precisely describe the achieved restoration level of supply for IEGS.

The rest of the paper is organized as follows: Section II studies the seismic impact on IEGS. Section III studies the overall operation scheme. A service index is presented in section IV. The test system and case study are in Sections VI and VII respectively. Section VIII concludes the paper.

## II. IMPACT EVALUATION OF SEISMIC STRESS

This section proposes a model to quantify system performance under seismic stresses. Load curtailment due to seismic stress is used as a metric to assess system functionality.

TABLE I RANGES OF PGA, PGV AND SEISMIC INTENSITY

Intensity	I	II ~	IV	V	VI	VII	VIII	IX
		III						
PGA	< 0.17	0.17-	1.4-	3.9-	9.2-	18-	34-	65-
(%g)		1.4	3.9	9.2	18	34	65	124
PGV	< 0.1	0.1-	1.1-	3.4-	8.1-	16-	31-	60-
(cm/s)		1.1	3.4	8.1	16	31	60	116

The relationship between seismic intensity and PGA, PGV can be classified by Table I [16]. In this table, seismic intensity range from I-IX is quantified by different PGA/PGV in %g and cm/s. For the gas network, the impact of seismic stress is

quantified by gas leakage, realized by the following steps: 1) Obtaining the number of damage points caused by a seismic stress based on (1). 2) Studying the condition of each damage point based on the EOD model in (2)-(7). 3) Calculating the overall gas leakage. For the electricity system, the seismic stress is quantified by electricity load losses in the following steps: 1) obtaining damage states and related probability of impacted lines. 2) calculating the damage expectation of CL of impacted lines with (8). 3) quantifying electricity load loss with (9).

## A. Fragility of Gas Networks

To study gas leakage caused by seismic stresses, the relationship between damage ratio and seismic intensity is classified. By representing the number of damage points of pipelines per kilometre, the model of damage rate for gas networks is applied. For pipes of ductile iron [17], the damage rate is

Damage rate = 
$$\frac{\text{Damage points}}{\text{Km}}$$
 = 0.00003 × (PGV)<sup>2.25</sup> (1)  
After relating the intensity of seismic activities to a certain

After relating the intensity of seismic activities to a certain damage ratio of gas networks, the leakage at each damage point can be quantified. Tis paper quantifies the leakage losses by investigating the equivalent orifice diameter (EOD) of damaged pipes. A leakage expectation based on EOD can be specified by the probability of various leakage scenarios.

Regarding buried pipelines, seismic stresses mainly cause five types of damage: annular disengagement, round crack, longitudinal crack, local crack of the pipe wall and local tear of the pipe wall. The EOD of damaged pipes considering different scenarios can be derived as [18],

$$d_1 = 2\sqrt{tkD} \tag{2}$$

$$d_2 = 2\sqrt{\theta}D\tag{3}$$

$$d_3 = 2\sqrt{LD\theta/\pi} \tag{4}$$

$$d_4 = 2\sqrt{k_1 k_2} D \tag{5}$$

$$d_5 = 2\sqrt{kwD} \tag{6}$$

Where  $d_1$ ,  $d_2$ ,  $d_3$ ,  $d_4$ ,  $d_5$  are the EOD under different damage scenarios in Table II, D is the diameter of damaged pipes,  $\theta$  is the opening angle, L is the length of the crack and can be taken as the length, w is the width of split and t, k,  $k_1k_2$  are constant set as  $10\sim16$  mm, 1% and 5% respectively. Because the opening angle  $\theta$  and width of split w are mainly determined by pipeline material, their values are set to  $0.1^{\circ}$  and 12 mm.

TABLE II
THE PROBABILITY OF LEAK SCENARIOS FOR PIPELINES OF

	VAR	IOUS MA	TERIALS [	[18]	
Pipe	Annular	round	longitu	Local	Local
Material	disenga	crack	dinal	loss of	tear of
	gement		crack	pipe	pipe
				wall	wall
Cast Iron	0.3	0.5	0.1	0.1	N/A
Ductile	0.8	N/A	0.1	0.1	N/A
Iron					
Riveted	0.6	N/A	0.3	0.1	N/A
Steel					
Welded	N/A	N/A	N/A	N/A	1.0
Steel					
Joint	1.0	N/A	N/A	N/A	N/A
Concrete					

The probabilities of 5 damage scenarios for different pipe materials are in Table II. For each material, the probability of possible damage scenarios is calculated. Subsequently, the overall expectation of EOD at a damage point is,

$$EOD = \sum_{i=1}^{n=5} P_i d_i \tag{7}$$

Where  $P_i$  is the probability of different leak scenarios,  $d_i$  is EOD under the five damage scenarios.

## B. Fragility of Electricity Systems

Seismic activities can cause four damage states of electricity lines, slight, moderate, extensive and complete. For a distribution branch, each damage state refers to a certain level of connection loss. The slight damage state refers to 4% connection loss (CL), moderate stage refers to 12% CL while extensive damage, complete damage represents 50% CL, 80% CL respectively. The detailed probability of each damage state is shown in Table III.

TABLE III
DAMAGE ALGORITHM FOR THE ELECTRICITY SYSTEM

Damage state	Median(g)	β
slight/minor	0.28	0.30
moderate	0.40	0.20
extensive	0.72	0.15
complete	1.10	0.15

To quantify the overall CL for different seismic intensities, the damage expectation should be determined. However, the four damage states are not completely independent. Because a more severe damage state contains lower severe damage stages, the damage expectation  $D_{CL}$  can be characterised as

$$D_{CL} = P_n C L_n + \sum_{i=2}^{n-1} (P_{CL,i-1} - P_{CL,i}) C L_{i-1}$$
 (8)

Where  $i \in [16 ..., n]$  represents four damage states.

For electricity systems, the final damage expectation describes the damage ratio of all lines.

## C. Load Curtailment

Load curtailment is mainly computed from two aspects: first, generation has insufficient capacity due to direct seismic impact or isolated branches. Secondly, when line outage occurs (including all types of circuit's damage), some branches can be overloaded or have reverse flow, load curtailment should be deployed to ease the burden. This scheme curtails load based on the demand sensitivity factor between branches and nodes.

The load curtailment is

$$L_{loss} = \sum_{k=1}^{n} (L_{line} + L_{pipe}) + \sum_{k=1}^{m} L_{gen} + L_{g,iso} + L_{e,iso} + L_{rev}$$
 (9)

Where, n is the number of overloaded lines, m is the number of decreased generation.  $L_{line}$ ,  $L_{pipe}$  ar related to the outage of electricity lines and gas pipes.  $L_{gen}$  is the load curtailment due to generation reduction.  $L_{g,iso}$  is the load curtailment due to isolated gas, and  $L_{e,iso}$  is the load curtailment due to isolated electricity circuitss.  $L_{rev}$  is the load curtailment due to reversed gas flow. All load curtailment is quantified by the sensitive factor of line outages based on PTDF.

## III. SYSTEM OPERATION STRATEGY

This section designs a combined operation and reconfiguration scheme to recover functionality by using

switches and gas valves. As damaged lines and pipes cannot be repaired in a short time, the dynamic load loss minimization before repair should be established according to load profiles and seismic variations. The operation of IEGS, storage units, and coupling components are conducted simultaneously to find the best reconfigure strategies.

# A. Integrated Operation of Electric Switches and Gas Valves

Assuming all branches are installed with switches/valves, then the system topology can be fully changed by switch/valve operation. Thus, an operation algorithm is developed in this section to maintain optimal solutions for system postcatastrophe topology.

The power flow equation can be expressed as,
$$V_{l}^{\dot{k}+1} = \frac{\frac{P_{l}-jQ_{l}}{\widehat{V_{l}k}} - \sum_{j=1}^{l-1} Y_{lj}\dot{V}_{j}^{k+1} - \sum_{j=l+1}^{n} Y_{ij}\dot{V}_{j}^{k}}{Y_{ii}}$$
(10)

Where, P<sub>i</sub> is the real power produced by the generator linked to bus i, Qi is the reactive power produced by the generator linked to bus i.

For gas networks, by assuming all pipes are installed with valves. The gas flow nodal balance equation is

$$AGA^TP + Q = 0 (11)$$

Where G is the admittance matrix of gas pipes, A is the connection matrix of the system, P is the pressure matrix of the gas system node, and Q is the flow rate vector of nodes.

The switch and valve operation is as below. Equation (12) is the objective function to maintain minimum energy loss based on switch/valve operation, (13) is the searching velocity's upgrade function, (14) is the searching location's upgrade function, (15) describes inertia weights, (16) is the sigmoid limiting transformation. Equations (17) and (18) refer to the voltage constraint and current constraint. Equation (22) is the parameter constraint and (23-24) are the searching location's constraints. Where *Pbest*<sub>i</sub> is the best position experienced by ith particle,  $Gbest_i$  is the best particle of the entire population ever achieved,  $V_i^t$  and  $x_i^t$  are the present velocity and position of particle i at the  $t^{th}$  iteration,  $\alpha$ ,  $\beta_1$  and  $\beta_2$  refer to inertia weights and weighting factors of the stochastic acceleration terms respectively,  $S(V_i)$  represents a transformation that can update particle velocity,  $r_1, r_2$  are numbers randomly chosen from a uniform distribution [0,1],  $V_c$  is the voltage constraint,  $I_c$ is the branch current constraint.,

$$Pbest_{i} = min\{\sum_{k=1}^{n} LL_{line} + \sum_{k=1}^{m} LL_{Buck} + LL_{iso} + \sum_{k=1}^{n} LL_{rev} + \sum_{k=1}^{m} LL_{demand}\}$$
(12)  

$$V_{i}^{t+1} = \alpha V_{i}^{t} + \beta_{1} r_{1} (Pbest_{i} - x_{i}^{t}) + \beta_{2} r_{2} (Gbest_{i} - x_{i}^{t})$$
(13)  

$$x_{i}^{t+1} = x_{i}^{t} + V_{i}^{t+1}$$
(14)  

$$\alpha^{t+1} = \alpha_{max} - t \times \frac{\alpha_{max} - \alpha_{min}}{t_{max}}$$
(15)  

$$S(V_{i}) = \frac{1}{1 + e^{-V_{i}}}$$
(16)

$$S(V_i) = \frac{1}{1 + e^{-V_i}} \tag{16}$$

$$V_{c,Min} \le V_c \le V_{c,Max} \tag{17}$$

$$I_{c.Min} \le I_c \le I_{c.Max} \tag{18}$$

$$DF_i^{t+1} \times DF_i^t \ge 0 \tag{19}$$

$$P_{c.min} \le P_c \le P_{c.max} \tag{20}$$

$$F_{c,Min} \le F_c \le F_{c,Max} \tag{21}$$

$$r_1, r_2 = rand\{0,1\}$$
 (22)

$$if \ r_1, r_2 < S(V_i(t+1)), x_i^{t+1} = 1$$
 (23)  
 $if \ r_1, r_2 > S(V_i(t+1)), x_i^{t+1} = 0$  (24)

$$if r_1, r_2 > S(V_i(t+1)), x_i^{t+1} = 0$$
 (24)

These variables can be adjusted to properly model gas networks. The constraints here are different from those for electricity systems: (19) prevents inversed pipeline flow, where  $DF_i^t$  represents the direction of pipeline j at time t, (20) describes the pressure constraint, where  $P_c$  refers to pipeline pressure, (21) is the flow constraint of pipes and  $F_c$  represents the gas flow of pipes.

The operation algorithm can find the best valve/switch operation that optimally decides closed lines/pipes and maximally avoids demand curtailment. The minimum curtailed load can be derived by maintaining properly closed lines/pipes and regulating reversed gas flows. The algorithm that searches for properly closed pipes starts from the pipes close to the pipe leak/crack.

# B. Electricity Storage

The energy level of storage at time step t+1, charging and discharging energies of the previous time step t can be described in (25). The battery energy level at the final time step is assumed to be equal to its initial level at the beginning of the optimization, as restricted in (27). Equations (26), (28)-(29) are the capacity operation constraints of electricity storage.

$$E_{ES}^{t+1} = E_{ES}^{t} - \mu_{Ech} P_{Ech}^{t} - P_{Edis}^{t} / \mu_{Edis}$$
(25)  

$$E_{ES}^{Min} \le E_{ES}^{t} \le E_{ES}^{Max}$$
(26)  

$$E_{ES}^{t} (t = 0) = E_{ES}^{t} (t = 24)$$
(27)  

$$0 \le P_{Edis}^{t} \le P_{ES}^{Max}$$
(28)  

$$-P_{ES}^{Max} \le P_{Ech}^{t} \le 0$$
(29)

$$E_{Fs}^{Min} \le E_{Fs}^t \le E_{Fs}^{Max} \tag{26}$$

$$E_{Fs}^t(t=0) = E_{Fs}^t(t=24)$$
 (27)

$$0 \le P_{Fdis}^t \le P_{Fs}^{Max} \tag{28}$$

$$-P_{ES}^{Max} \le P_{Ech}^t \le 0 \tag{29}$$

Where  $\mu_{Ech}$  describes the charging efficiency of electricity storage units and  $\mu_{Edis}$  is the discharging efficiency.

## C. Gas Storage

Natural gas storage serves as an adjustable supply/demand entity when gas well capacity or pipeline transmission cannot guarantee supply security. It is assumed that natural gas storage units can discharge to support external systems, but the directions of pipeline flow are fixed. Storage energy level constraint is in (32). Gas storage charging /discharging constraint is in (30) and capacity operation constraints are described in (31) and (33)-(34).

$$E_{GS}^{t+1} = E_{GS}^{t} - \mu_{Gch} P_{Gch}^{t} - P_{Gdis}^{t} / \mu_{Gdis}$$
(30)  

$$E_{GS}^{Min} \leq E_{GS}^{t} \leq E_{GS}^{Max}$$
(31)  

$$E_{GS}^{t} (t = 0) = E_{GS}^{t} (t = 24)$$
(32)  

$$0 \leq P_{Gdis}^{t} \leq P_{GS}^{Max}$$
(33)  

$$-P_{GS}^{Max} \leq P_{Gch}^{t} \leq 0$$
(34)

$$E_{Gs}^{Min} \le E_{Gs}^t \le E_{Gs}^{Max} \tag{31}$$

$$E_{Gs}^t(t=0) = E_{Gs}^t(t=24)$$
 (32)

$$0 \le P_{Gdis}^t \le P_{Gs}^{Max} \tag{33}$$

$$-P_{Cs}^{Max} \le P_{Cch}^t \le 0 \tag{34}$$

Similar to the electricity system,  $\mu_{Gch}$  describes its charging efficiency of gas storage and  $\mu_{Gdis}$  is its discharging efficiency.

## D. SOP

Equation (35) describes the voltage deviation offered by SOP.

$$f_{dev} = \sum_{i=1}^{N_I} |U_{t,i}^2 - 1| \ (U_{t,i} \ge U_{Max} || U_{t,i} \le U_{Min}) \ (35)$$

Where  $U_{t,i}$  is the voltage of node i at time t,  $U_{Max}$  and  $U_{Min}$  are

the voltage constraints.

# E. Coupling Units Operation

This section models the operation and constraints of coupling units, including SOP, electrolyser and CHP. Equations (36) and (39) represent the time-varying energy conversion electrolyser and CHP, (37)(38) and (40)(41) describe the input/output limits and capacity constraints for electrolyser and CHP respectively.

## 1) Electrolyser

$$V_e(t) = \eta e \times \frac{P_e(t)}{t}$$
 (36)

$$V_e(t) = \eta e \times \frac{P_e(t)}{HHV}$$

$$\underline{GL_{i,Min}} \le E_{PtG,i} \le \overline{EL_{i,Max}}$$
(36)

$$PtG_{Min} \le E_{PtG} \le \overline{PtG_{Max}}$$
 (38)

# 2) CHP

$$PH_e(t) = \eta H \times PH_g(t)$$
 (39)

$$GL_{Min} \le E_{GtP} \le \overline{EL_{Max}}$$
 (40)

$$GtP_{Min} \le E_{GtP} \le \overline{GtP_{Max}}$$
 (41)

Where  $P_e$  is the power consumed by the electrolyser,  $\eta e$  is its electrical efficiency, and HHV is the higher heat value of  $H_2$ .  $\eta H$  is the efficiency of CHP,  $PH_q$  represents gas input.

#### IV. SERVICE INDEX

In this paper, service index R in (42) is obtained by comparing the loading level under normal and stressful conditions of the whole system. Subsequently, the slope and reduction of loading level represent the recovering/reduction rate and load loss respectively. Subsequently, R index can reflect the integral of load level in terms of time, which is directly related to load loss and recovery time.

$$R = \sum_{1}^{N} P_{f,n} \times \frac{\int_{0}^{T_{0}} NL(t)dt - RS_{n}}{\int_{0}^{T_{0}} NL(t)dt}$$
(42)

Where, N is the number of failure scenarios,  $P_{f,n}$  describes the failure probability of scenario n,  $T_0$  is the period of seismic duration, NL(t) is the normal load level,  $RS_n$  is the area of actual load level along with time series.

Thus, this paper sets the objective of the reconfiguration algorithm to maximize the service index. The objective function of the overall problem is as follows,

$$Max Service Index = R_{Phest}$$
 (43)

$$Pbest = min\{Pbest_i + Pbest_i\}$$
 (44)

$$(E_{PtG,1}||E_{PtG,2})\&\&(E_{GtP}) = 1$$
 (45)

Where (43) is the objective function,  $R_{Pbest}$  refers to the service index when the switches and valves are operated according to Pbest. Equation (45) is the operational constraints of CHP and electrolysers.

# V. IMPLEMENTATION

Fig. 1 shows the implementation steps of the proposed system reconfiguration and operation method.

The implementation steps are as follows:

a) Based on the proposed model, the seismic intensity is quantified by PGA and PGV.

- b) It is to calculate the damage expectation of the electricity system. It then quantifies the load curtailment caused by line overloading, generation output reduction, and isolated subcircuits based on (9).
- Based on EOD and damage rate, the pressure loss/gas loss of pipes can be obtained. For the electricity system, the system loss is described by applying different fragility curves. Consequently, overall load curtailment and related R loss can be determined.
- d) To improve the service index, a searching algorithm is applied to find the most proper reconfiguration scehmes by finding the max service index.
- Finally, the method stops when the maximum service restoration is found. To evaluate the rationality of the proposed method, system restoration achieved by dynamic operation algorithm and single operation is compared.

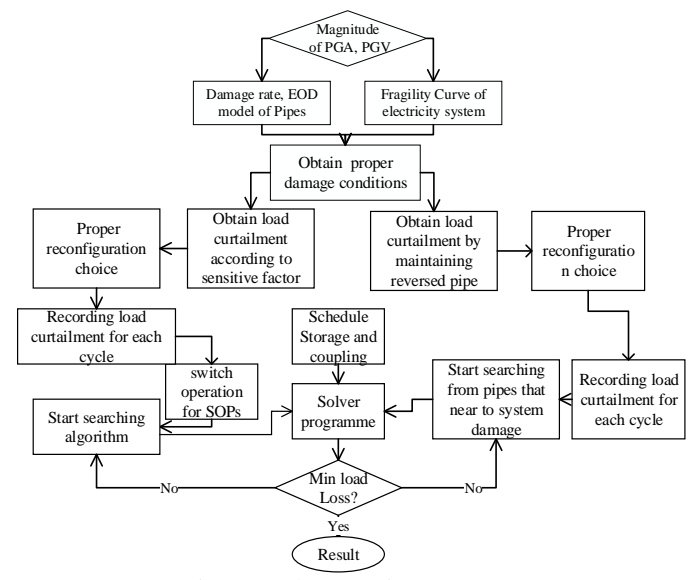


Fig. 1 Implementation steps

#### VI. TEST SYSTEM

As shown in Fig. 2, the test system contains 33 buses, 2 electrolysers, a CHP and 5 SOPs. An electric storage device is placed at bus 22 while a gas storage is installed at node 35. The initial switch operation would be 32 switches normally closed and 5 switches normally opened. In Fig. 2, the dash lines represent soft open points where the lines between 33 and 46, 18 and 35 are equipped with electrolysers. Branch 39-2 is facilitated by the CHP. Subsequently, it is assumed that the seismic stress and following aftershocks would damage the system twice. The seismic activity and aftershocks would happen at the time of 13:30 and 17:30 respectively.

In this section, the sampled seismic intensity and the first aftershock is set to VII and VI respectively. The subsequent aftershock would be seen as harmless to the system. Thus PGA is 0.25%g (aftershock 0.18g) and PGV is 31 cm/s. the damage expectation of CL is then classified as 3% of 37 branches (1.11), which indicates the number of failed transmission lines is 1. Similarly, the aftershock would lead to a failure line as well. For the seismic intensity of 31 cm/s, the damage rate among the gas network is determined as 0.0068. If the overall length of gas pipes is 15 km, there will be 1 damage point. The locations of gas leaks are randomly generated among all gas pipelines. Assume all pipes within the gas network are constructed by Ductile Iron, based on the probabilities of that 5 damage scenarios, the damage expectation of EOD can then be estimated as 3cm. Subsequently, system leakage loss due to seismic damage is quantified based on *Pipeline Studio*, a pipeline analysis software that can model a wide range of steady-state and transient analysis of pipe systems. Based on the Benedict-Webb-Rubin equation, the hydraulic analysis function of the natural gas pipeline is employed.

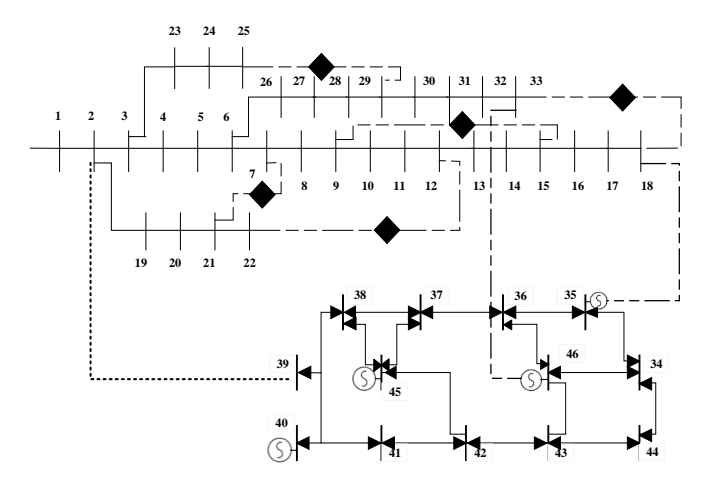


Fig. 2 The test system

A dynamic load profile is developed based on seasons, occupants, and house type. Five classifications, including 3 electricity and 2 heat load profiles, are simulated as Figure 3. The load of buses 1-18, buses 19-25, and the rest of buses, are assumed to follow the first, second, and third load profile respectively. The load of gas nodes with odd serial numbers are assumed to vary according to the first space heating profile while nodes with even serial numbers follow the second heating profile. For the couplings between the two systems, the CHP would always be switched on with adjustable output in response to the electrical demand. In this paper, the load profiles are assumed to generate for winter weekdays.

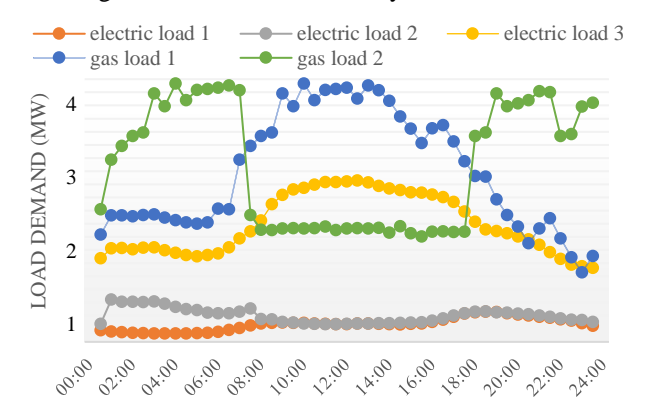


Fig. 3 Time-series load profiles for 5 types of load

Regarding seismic stress, branch 28-29 and pipe 2 are chosen to be damaged by seismic stress at 13:30. The state of the test system would become 1 switched offline, 1 switched off pipe,

with 5 SOPs not in use, which can be regarded as the initial searching point of the searching algorithm. Then, at 17:30, branch 12-13 is damaged and switched off. The algorithm is implemented to search for optimal switch/valve operations to minimize recovery time and loss load.

The gas network could be assumed to be immune from the aftershock (damage point <1). Thus, in the final results, there would be 5 switches, 1 valve off (including SOPs not in use and the damaged branches), but the number of pipes that would be closed is not fixed. Assuming the number of reconfiguring operations for the test system within one day is 5, to address the large load loss according to sharp demand variations, the triggered time would be at 1:30, 8:30, 11:30, 17:30 and 20:30, according to the load profile.

#### VII. CASE STUDY

In this section, the restoration results of A) Dynamic Reconfiguration with Multi Operations B) Conventional Reconfiguration with Multi Operations C) Conventional Reconfiguration with Single Operation would be compared. In the single operation, system units (e.g. energy storages, SOPs, CHPs and electrolysers) are only operated/reconfigured once after the seismic activities. In multi operations, dynamic reconfiguration/operation, triggered by load variation and aftershocks are applied.

# A. Dynamic Reconfiguration with Multi Operations

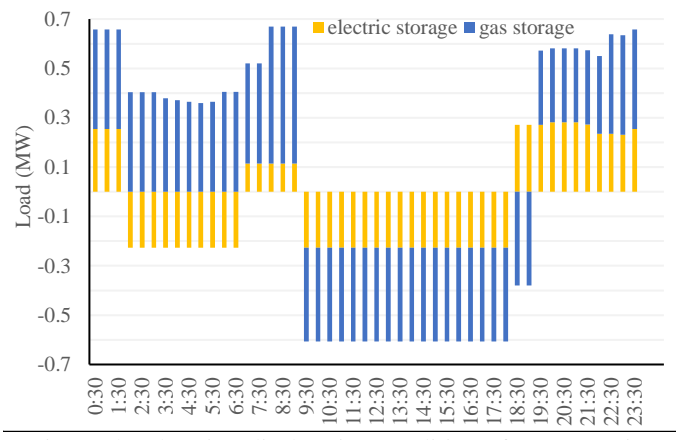
In this section, both dynamic reconfiguration and dynamic operation would be deployed, the service index at time 1:30 (damage line 28-29) and 17:30 (damage line 12-13, 28-29) would be 0.554 and 0.306 respectively.

Table IV shows that, at 1:30, the system is reconfigured to a structure that only applies one SOP, in that case only the damaged branch 28-29 is switched off. The percentage of enhanced resilience compared with the original system would be 44.04% at that time. At 8:30 when the load of buses 26-33 increases rapidly, the reconfiguration choice would be to switch off the SOP in 25-29, and switch on SOP 18-33. Subsequently, since the load slightly changes in 3 hours, the reconfigured solution at 11:30 approximately remains the same. In other words, there is no need for an extra reconfiguration at 11:30. The efficiency of resilience enhancement at this time period is still regarded as 48.27%. At 17:30 when branch 12-13 is damaged by varied wind stress and the demand for buses 26-33 starts to decrease, the switched-off branches are 12-13 and 28-29, while SOP 9-15 and 18-33 are turned on, leading to an efficiency of 29.57%. Lastly, when the demand of buses 26-33 drops back to a lower stage at 20:30, branches 11-12, 12-13 and 28-29 are turned off while SOP 12-22, 18-33 and 25-29 are turned on. The efficiency would be 34.28%.

Fig. 4 shows the power output of system energy storage units in scenario 1, where positive and negative outputs respectively indicate discharging and charging the storage units. It can be seen that the charging cycle of the electric storage is from 1:30 to 6:30 and 8:30 to 17:30 while its discharging cycle is from 0:00 to 1:30, 6:30 to 8:30 and 17:30 to 0:00. Referring to system recovering and loss load mitigation, the second discharging

cycle can be related to increasing load demand while the third discharging cycle is determined by the significant load loss among branch 19-22. For the gas storage unit, the discharging cycle occurs from 18:30 to 8:30 and the charging cycle is between 8:30 to 18:30. Because there is only 1 charging/discharging cycle of the gas storage unit, it can be concluded that when the gas system is immune to an extreme event, only variational load demand can affect its system topology and the whole reconfiguration process can be seen as arranging it to support the electricity system.

	TABLE IV			
RECONFIGURAT	TION RESULTS FOR THE ELECT	TRICITY SYSTEM		
	1:30			
	Before Re	After Re		
off mode branches	28-29, 8-21, 9-15, 12-22, 19- 33, 25-29	28-29, 8-21, 9-15, 12- 22, 18-33		
In used SOPs Resilience index	0.554	25-29 0.798		
Resilience				
enhancement	44.049	%		
	8:30			
	Before Re	After Re		
off mode branches	28-29, 8-21, 9-15, 12-22, 19- 33, 25-29	28-29, 8-21, 9-15, 12- 22, 25-29		
In used SOPs		18-33		
Resilience index	0.549	0.814		
Resilience enhancement	48.279	%		
emianeement	11:30			
	Before Re	After Re		
off mode branches	28-29, 8-21, 9-15, 12-22, 19- 33, 25-29	28-29, 8-21, 9-15, 12- 22, 25-29		
In used SOPs		18-33		
Resilience index	0.815	0.815		
Resilience enhancement	N/A			
emancement	17:30			
	Before Re	After Re		
off mode branches	12-13, 28-29, 8-21, 9-15, 12- 22, 19-33, 25-29	12-13, 28-29, 8-21, 9- 15, 12-22		
In used SOPs	22, 17 33, 23 27	9-15, 18-33		
Resilience index	0.306	0.482		
Resilience	29.579	%		
enhancement	20:30			
		A.C. D		
off mode branches	Before Re 12-13, 28-29, 8-21, 9-15, 12-	After Re 12-13, 28-29, 11-12, 8-		
In and COD.	22, 19-33, 25-29	21, 9-15		
In used SOPs Resilience index	0.318	12-22, 18-33, 25-29 0.427		
Resilience index				
enhancement	34.28%			



enhancement

Fig. 4 The charging/discharging condition of storage units

	IABLE V	
RECONFIGURATIO	N RESULTS FOR	GAS NETWORK

	1:30	
	Before Re	After Re
off mode Pipes	Pipe 2	Pipe 2, 9
Reversed pipes	9	N/A
Resilience index	0.652	0.715
Resilience		9.66%
enhancement		2.0070
	8:30	
	Before Re	After Re
off mode Pipes	Pipe 2	Pipe 2, 15
Reversed pipes	15	N/A
Resilience index	0.627	0.853
Resilience enhancement		36.04%
emancement	11:30	
	Before Re	After Re
off mode Pipes	Pipe 2	Pipe 2, 12
Reversed pipes	12, 15	N/A
Resilience index	0.471	0.464
Resilience		-1.49%
enhancement		-1.4970
	17:30	
	Before Re	After Re
off mode Pipes	Pipe 2	Pipe 2
Reversed pipes	N/A	N/A
Resilience index	0.597	0.584
Resilience enhancement		-2.18%
	20:30	
	Before Re	After Re
off mode Pipes	Pipe 2	Pipe 2, 9, 12
Reversed pipes	9, 12, 15	N/A
Resilience index	0.443	0.765
Resilience enhancement		72.69%

For the gas network, Table V shows that reversed pipe flow would be triggered by the loss of pipeline 2. Thus, the gas network can not be only operated to fully support the electric system, it needs to prevent reversed pipe flow and minimize loss load. At 1:30, although the two types of load demand remain stable, the second class of load is 3 times higher than the first load type. The reversed gas flow appears in pipe 9, and after the closure of valves in pipes 2 and 9, the curtailed load can be slightly recovered as 9.66%. Then, at 8:30, the pipe closure driven by the reconfiguration would be pipe 2, 12. Moreover, the operation for the reversed pipe 15 would trigger much more load loss reduction, which leads to more resilience enhancement.

During lunchtime, the first type of load reaches its peak value and trends to be stable, and the other type of load stays at a low level. It can be seen that the reversed gas flows appear in pipes 12, 15. According to the reconfiguration algorithm, the best solution would be further closing valves in pipe 12 to prevent the reversion of pipes 12,15. However, the efficiency is around -1.49%, which means to prevent reversed pipes load demand should be further curtailed. At 17:30, the first type of load demand decreases while the second type of demand rapidly grows. At this time only pipe 2 gets reversed. The two types of load maintain with similar variations at the final time step, the reversed gas flows are in pipes 9, 12, 15. If valves in pipes 9, 12 are closed and load curtailment is used to prevent the reverse flow of pipe 15, the load loss would be reduced by 72.69%.

Thus, the overall service enhancement for the electricity system is 39.28%, while for the gas network it only has an

enhancement of 22.94%. The overall enhancement efficiency is 25.97%.

### B. Conventional Reconfiguration with Multi Operations

In this scenario, reconfiguration would only be operated once while system components' repeated actions are allowed to recover the system under branches 12-13, 28-29 and pipe 2's damage. In Table III, it can be seen that although components such as energy storage units, CHP and electrolysers are allowed to be operated multiple times, the system can only be enhanced by 23.20%. The reason for this relatively low efficiency can be related to the limitation of its original topological structure.

TABLE VI

RECONFIGURATION	RECONFIGURATION RESULTS FOR THE OVERALL SYSTEM					
`	Before	After				
	Reconfiguration	Reconfiguration				
Switched off branches	12-13, 28-29	12-13, 28-29, 25-29,				
		18-33				
In used SOPs	N/A	8-21, 9-15, 12-22				
Resilience index	0.306	0.377				
Overall enhancement	N/A	23.20%				

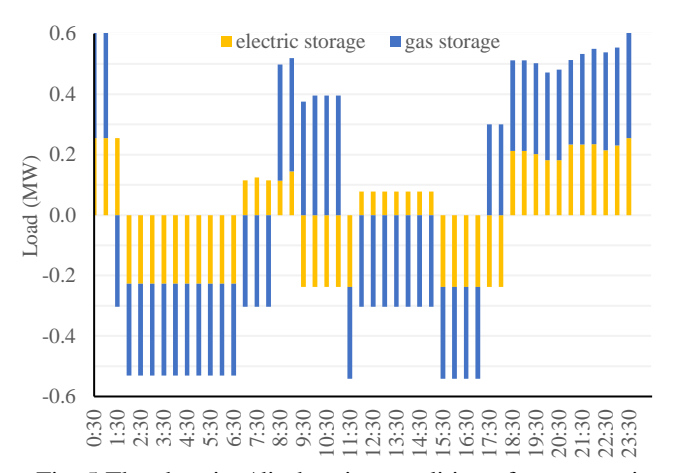


Fig. 5 The charging/discharging condition of storage units

TABLE VII

	COMPUTATIONAL RESULTS FOR THE INTERFACE UNITS					
Time`	$CHP_A$	$Ele1_A$	$Ele2_A$	$CHP_B$	$Ele1_{B}$	$Ele2_B$
0:30	0.43	0.12	0.14	0.43	0.16	0.17
1:30	0.42	0.08	0.11	0.42	0.17	0.18
8:30	0.31	0.11	0.12	0.45	0.19	0.18
11:30	0.39	0.16	0.17	0.47	0.16	0.16
17:30	0.42	0.2	0.2	0.46	0.17	0.18
20:30	0.47	0.18	0.2	0.47	0.18	0.16
0:30	0.43	0.12	0.14	0.43	0.16	0.17

For scenario 2, the operation of system energy storage is shown in Fig.5. It can be seen that the discharging cycle of the electric storage is from 0:00 to 1:30, 6:30 to 9:30, 11:30 to 15:30 and 17:30 to 0:00 while its charging cycle is from 1:30 to 6:30, 8:30 to 11:30 and 15:30 to 17:30. As for the gas storage, the discharging cycle occurs from 18:30 to 1:30 and 8:30 to 11:30 and the charging cycle is between 1:30 to 8:30 and 11:30 to 17:30. Additionally, the operation results of interface units in scenario A/B are shown in Table VII. Consequently, it is seen that the storage and interface units are more frequently operated

to offer loss load mitigation and restore system functionality when the reconfiguration can only be applied once.

### C. Conventional Reconfiguration with Single Operation

In this scenario, reconfiguration and system components would only be operated once to recover the system under branch 12-13 28-29 and pipe 2's damage.

RECONFIGURATION RESULTS FOR THE OVERALL SYSTEM

	Before Reconfiguration	After Reconfiguration
Switched off branches	12-13, 28-29	12-13, 28-29, 9-15, 18-
		33
In used SOPs	N/A	8-21, 12-22, 25-19
Overall Storage units	0	0.81
supply (MW)		
Resilience index	0.306	0.354
Resilience enhancement	N/A	17.64%

Table VIII shows the results after the recovery of the whole system. Three SOPs 8-21, 12-22 and 25-19 are activated and the total supply of gas/electricity storage is 0.81 MW. The structure of this reconfigured system is slightly different from the previous solution but still maintains a radial structure. Although nearly all types of load trends to drop at the final time step, the related load loss is still relatively high due to the constraint of system structure. Thus, the overall enhancement efficiency is 17.64%.

Other natural events could have a direct negative impact on energy systems: icing may cause conductor galloping and breaking, pole leaning/collapse, or insulator flashover. Extreme temperature would lead to the variation of load demand, and sometimes generator outages. Snow and precipitation mainly trigger cascading failures. These events will be investigated in our future work.

# VIII. CONCLUSION

This paper proposes a combined scheme to enhance the resilience of integrated energy systems against seismic events, based on reconfiguration and smart system operation. Through the extensive case study, the key findings are:

- Compared to conventional reconfiguration, the combined dynamic reconfiguration method with smart operation can offer more significant resilience enhancement.
- Both recovery time and system loss can be mitigated by smart operations together with multi reconfiguring the integrated energy system.
- The proposed method for the gas network enhancement can effectively prevent the reversed gas pipes. However, the proposed method sometimes it can even cause the service index to decrease, which need further research.

The work provides system operators with a powerful tool to restore the service of integrated energy systems under extreme seismic events with reduced load loss. The framework can also be applied to other natural events that can impact IEGS, helping system operators ensure supply security in the decarbonisation.

#### REFERENCES

- [1] M. Gil, P. Duenas, J. Reneses, Electricity and Natural Gas Interdependency: Comparison of Two Methodologies for Coupling Large Market Models Within the European Regulatory Framework, IEEE transactions on power systems, 31 (2016) 361-369.
- [2] M. Qadrdan, J. Wu, N. Jenkins, J. Ekanayake, Operating Strategies for a GB Integrated Gas and Electricity Network Considering the Uncertainty in Wind Power Forecasts, IEEE transactions on sustainable energy, 5 (2014) 128-138.
- [3] Z. Zeng, Reliability Evaluation for Integrated Power-Gas Systems With Power-to-Gas and Gas Storages, IEEE Transactions on Power Systems, 35 (2020) 571-584.
- [4] Y. Ding, C. Singh, L. Goel, J. Østergaard, P. Wang, Short-Term and Medium-Term Reliability Evaluation for Power Systems With High Penetration of Wind Power, IEEE Transactions on Sustainable Energy, 5 (2014) 896-906.
- [5] M. Bao, Y. Ding, C. Singh, C. Shao, A Multi-State Model for Reliability Assessment of Integrated Gas and Power Systems Utilizing Universal Generating Function Techniques, IEEE transactions on smart grid, 10 (2019) 6271-6283.
- [6] K. Poljanšek, F. Bono, E. Gutiérrez, GIS-based method to assess seismic vulnerability of interconnected infrastructure: A case of EU gas and electricity networks, Office for Official Publications of the European Communities, 2010. [7] L. Dueñas Osorio, J.I. Craig, B.J. Goodno, Seismic response of critical
- interdependent networks, Earthquake engineering & structural dynamics, 36 (2007) 285-306.
- [8] K. Poljanšek, F. Bono, E. Gutiérrez, Seismic risk assessment of interdependent critical infrastructure systems: the case of European gas and electricity networks, Earthquake Engineering & Structural Dynamics, 41 (2012) 61-79.
- [9] K.P. Schneider, F.K. Tuffner, M.A. Elizondo, C.-C. Liu, Y. Xu, D. Ton, Evaluating the feasibility to use microgrids as a resiliency resource, IEEE Transactions on Smart Grid, 8 (2016) 687-696.
- [10] Z. Wang, J. Wang, Self-healing resilient distribution systems based on sectionalization into microgrids, IEEE Transactions on Power Systems, 30 (2015) 3139-3149.
- [11] Y. Tan, F. Qiu, A.K. Das, D.S. Kirschen, P. Arabshahi, J. Wang, Scheduling post-disaster repairs in electricity distribution networks, IEEE Transactions on Power Systems, (2019).
- [12] Y. Shen, C. Gu, Z. Ma, X. Yang, P. Zhao, A Two-Stage Resilience Enhancement for Distribution Systems Under Hurricane Attacks, IEEE Systems Journal, (2020).
- [13] X. Liu, M. Shahidehpour, Z. Li, X. Liu, Y. Cao, Z. Bie, Microgrids for enhancing the power grid resilience in extreme conditions, IEEE Transactions on Smart Grid, 8 (2016) 589-597.
- [14] P. Dehghanian, B. Zhang, T. Dokic, M. Kezunovic, Predictive risk analytics for weather-resilient operation of electric power systems, IEEE Transactions on Sustainable Energy, 10 (2018) 3-15.
- [15] P. Dehghanian, S. Aslan, P. Dehghanian, Quantifying power system resiliency improvement using network reconfiguration, in: 2017 IEEE 60th International Midwest Symposium on Circuits and Systems (MWSCAS), IEEE, 2017, pp. 1364-1367.
- [16] D.J. Wald, V. Quitoriano, T.H. Heaton, H. Kanamori, Relationships between peak ground acceleration, peak ground velocity, and modified Mercalli intensity in California, Earthquake spectra, 15 (1999) 557-564.
- [17] FEMA, Multi Hazard Loss Estimation Methodology Earthquake Model: HAZUS MR4 Technical Manual, (2004).
- [18] P. Shi, T.D. O'Rourke, Seismic response modeling of water supply systems, (2006).

**Yichen Shen** received the B.Eng. degrees in Electrical and Electronic Engineering from the University of Bath, U.K., and in Electrical Power Engineering from North China Electric Power University, China, both in 2017. Then, he received the Ph.D degree from the University of Bath, U.K. His research interest is resilient multi energy systems.

Chenghong Gu (Member, IEEE) received the bachelor's and master's degree in electrical engineering from Shanghai University of Electric Power and Shanghai Jiao Tong University, Shanghai, China, in 2004 and 2007, and the Ph.D. degree in electrical engineering from the University of Bath, Bath, U.K., in 2010. He worked with DECC U.K. to quantify the value of demand response to the energy system under 2050 pathways. He has been involved in the design

of the network pricing method—long-run incremental cost pricing (LRIC) for Western Power Distribution, which has been adopted by the wide U.K. power industry. He was an EPSRC Research Fellow with the University of Bath. He is a Reader with the Department of Electronic and Electrical Engineering, University of Bath. His major research interests are power economics and markets, multivector energy systems, smart grid planning, and operation. Dr. Gu is a Subject Editor for the IET Smart Grid.

Yue Xiang (Senior Member, IEEE) received the B.S. and Ph.D. degrees in electrical engineering from Sichuan University, China, in 2010 and 2016, respectively. From 2013 to 2014, he was a joint Ph.D. Student with the Department of Electrical Engineering and Computer Science, University of Tennessee, Knoxville, TN, USA, a Visiting Scholar with the Department of Electronic and Electrical Engineering, University of Bath, Bath, U.K., in 2015, and also a Visiting Researcher with the Department of Electrical and Electronic Engineering, Imperial College London, London, U.K., in 2019–2020. Now he is an Associate Professor with the College of Electrical Engineering, Sichuan University, Chengdu, China. His main research interests include distribution network planning and optimal operation, power economics, electric vehicle integration, and smart grids.

Yang Fu received the Ph.D. degree in electrical engineering from Shanghai University, Shanghai, China, in 2007. Currently, he is a Professor and Head of Shanghai University of Electric Power, Shanghai, China. His research interest includes power system analysis and new energy planning and optimization.

**Da Huo** received the B.Eng. degrees in Electrical and Electronic Engineering from the University of Bath, U.K., and in Electrical Power Engineering from North China Electric Power University, Baoding, China, both in 2014. He received the Ph.D. degree from the University of Bath, U.K., in 2018. He is currently a research associate with the School of Engineering, Newcastle University. His main research interests are distribution systems and whole energy systems.

**Junlong Li** received the B.Eng. degree in College of Electrical Engineering from Sichuan University, Chengdu, China, in 2015 and 2019. He is currently pursuing the Ph.D. degree in electronic and electrical engineering at the University of Bath. His main research interests include edge-cloud computing in power systems, energy management system, energy system economics.

Pengfei Zhao was born in Beijing, China. He received the double B.Eng. degree from the University of Bath, U.K., and North China Electric Power University, Baoding, China, in 2017. He received the Ph.D degree from the University of Bath, U.K. He was a visiting Ph.D. student at Smart Grid Operations and Optimization Laboratory (SGOOL), Tsinghua University, Beijing, China in 2019. Dr. Zhao is currently an Assistant Professor at the State Key Laboratory of Management and Control for Complex Systems, Institute of Automation, Chinese Academy of Sciences. His major research interests include the intelligent decision-making of low-carbon energy systems and social computing.